NeuroImage 146 (2017) 236–245

Contents lists available at ScienceDirect

NeuroImage

journal homepage: www.elsevier.com/locate/neuroimage

Spatiotemporal characteristics of sleep spindles depend on cortical location

Giovanni Piantoni[a,b,*], Eric Halgren[c], Sydney S. Cash[a,b]

[a] Massachusetts General Hospital, Boston, MA, United States
[b] Harvard Medical School, Boston, MA, United States
[c] University of California San Diego, La Jolla, CA, United States

ARTICLE INFO

Keywords:
Sleep
Spindles
Local
Co-occurrence
Propagation

ABSTRACT

Since their discovery almost one century ago, sleep spindles, 0.5–2 s long bursts of oscillatory activity at 9–16 Hz during NREM sleep, have been thought to be global and relatively uniform throughout the cortex. Recent work, however, has brought this concept into question but it remains unclear to what degree spindles are global or local and if their properties are uniform or location-dependent. We addressed this question by recording sleep in eight patients undergoing evaluation for epilepsy with intracranial electrocorticography, which combines high spatial resolution with extensive cortical coverage.

We find that spindle characteristics are not uniform but are strongly influenced by the underlying cortical regions, particularly for spindle density and fundamental frequency. We observe both highly isolated and spatially distributed spindles, but in highly skewed proportions: while most spindles are restricted to one or very few recording channels at any given time, there are spindles that occur over widespread areas, often involving lateral prefrontal cortices and superior temporal gyri. Their co-occurrence is affected by a subtle but significant propagation of spindles from the superior prefrontal regions and the temporal cortices towards the orbitofrontal cortex.

This work provides a brain-wide characterization of sleep spindles as mostly local graphoelements with heterogeneous characteristics that depend on the underlying cortical area. We propose that the combination of local characteristics and global organization reflects the dual properties of the thalamo-cortical generators and provides a flexible framework to support the many functions ascribed to sleep in general and spindles specifically.

Introduction

The cortical extent and spatiotemporal dynamics of spontaneous oscillatory rhythms are fundamental principles of brain organization and the object of intense investigation. This is particularly true for oscillations occurring during sleep. One such canonical oscillation is the spindle, a 0.5–2 s long burst of oscillatory activity between 9 and 16 Hz (Davis et al., 1937; De Gennaro and Ferrara, 2003). These graphoelements arise from the interaction of distinct populations of thalamic and cortical neurons (Steriade et al., 1993a) and are thought to represent a common mechanism for many functions attributed to sleep, such as memory consolidation (Diekelmann and Born, 2010; Fogel and Smith, 2011; Lüthi, 2013) and synaptic plasticity (Rosanova and Ulrich, 2005). Putative sources of spindle activity have been identified in lateral frontal and superior parietal regions (Anderer et al., 2001; Gumenyuk et al., 2009; Manshanden et al., 2002; Siclari et al., 2014; Urakami, 2008), but their presence in other regions, especially in the temporal lobe, has been subject of long-running debates (Montplaisir et al., 1981; Peter-Derex et al., 2012; Sarasso et al., 2014).

Pioneering work indicated that spontaneous spindles during natural sleep and barbiturate anesthesia are synchronized over large cortical areas (Achermann and Borbély, 1998; Contreras et al., 1997), This observation has been supported by studies combining electroencephalogram (EEG) and fMRI showing regional but widespread activation associated with spindles (Andrade et al., 2011; Schabus et al., 2007). More recent studies based on magnetoencephalography (MEG) and intracranial EEG (iEEG) in patients with epilepsy, however, have advanced the notion that spindles are a fundamentally isolated event (Andrillon et al., 2011; Dehghani et al., 2010b; Frauscher et al.,

Abbreviations: ANOVA, analysis of variance; CT, cortical tomography; ECoG, electrocorticography; EEG, electroencephalogram; FDR, false discovery rate; iEEG, intracranial EEG; LMEM, linear mixed-effects regression model; MEG, magnetoencephalography; MRI, magnetic resonance imaging; NREM, non-rapid eye movement; ReML, Restricted Maximum Likelihood

* Correspondence to: Department of Neurology, Massachusetts General Hospital, 55 Fruit St, Boston, MA 02114, United States.
E-mail address: gio@gpiantoni.com (G. Piantoni).

http://dx.doi.org/10.1016/j.neuroimage.2016.11.010
Received 23 June 2016; Accepted 5 November 2016
Available online 11 November 2016
1053-8119/

2015; Nir et al., 2011; Sarasso et al., 2014). However, the sparse sampling and the high spatial selectivity of depth electrodes in iEEG might bias towards spatially limited phenomena, and the true spatial extent of spindles remains unknown.

In fact, the degree to which spindles manifest themselves on the scalp as local or widespread events might depend on the underlying cortical regions, which vary in terms of corticocortical and thalamocortical connectivity. This issue is linked to the observation that distant brain regions are associated with varying spindle characteristics, such as density, amplitude, and duration (Martin et al., 2013). This is particularly evident for the distinction between fast and slow spindles, with a lower peak in the spindle frequency band for more anterior electrodes (De Gennaro and Ferrara, 2003; Gibbs and Gibbs, 1950; Jobert et al., 1992).

The dichotomy between global and local events becomes less tenable if we consider the proposal that spindles represent a mixture of different types of phenomena – some which might be exquisitely focal while others are more broadly spread, depending on the degree to which thalamic pathways, core or matrix, contribute to their generation (Bonjean et al., 2012; Dehghani et al., 2010a,b). Reconciling these viewpoints may be aided by the examination of the spatial extent and the synchronization properties of sleep spindles by recording techniques that offer both fine-grained spatial resolution and broad cortical coverage, such as electrocorticography (ECoG), in which grids of electrodes are placed directly on the cortical surface.

In the current study, we investigated fundamental questions regarding the spatial properties of the sleep spindle from continuous ECoG recordings in patients with epilepsy who were candidates for resective surgery. We detected spindles in individual channels during non-rapid eye movement (NREM) sleep in eight participants and mapped their characteristics onto the underlying cortical structures. We investigated three questions: Can the sleep spindle be considered a uniform phenomenon at the cortical level based on the spatial variability of its fundamental characteristics, such as the peak frequency in the spindle frequency band, its amplitude, and its duration? Should the spindle be thought of as a local or a global phenomenon based on their spatial extent and synchronization profile? Is there a preferential direction in the propagation of these events, akin to the bias for anterior-to-posterior propagation of slow waves and K-complexes (Mak-McCully et al., 2015; Massimini et al., 2004)?

Materials and methods

ECoG recordings

Recordings were obtained from eight patients with drug-resistant epilepsy implanted semi-chronically with a grid of electrodes on the pial surface in an effort to localize the seizure origin (see patients' characteristics in Table 1). The grids consisted of platinum-iridium electrodes of 3 mm diameter spaced 10 mm apart (Ad-Tech Medical Instrument Corp., Racine, WI). One strip of electrodes positioned in the epidural space facing the skull was used as reference during the recordings. Due to the craniotomy and the risk of infection, no external electrodes was applied on the scalp. Recordings were performed with clinical EEG monitoring equipment (XLTEK, Natus Medical Inc., Pleasanton, CA) and sampled at 500 Hz, 512 Hz, or 1024 Hz. The research was approved by the local institutional review board and electrode placement was determined solely by clinical criteria.

Nights that did not have any seizures in the preceding or following 12 h were scored visually by an expert rater from the ECoG electrodes following as closely as possible the standard sleep stage classification (Iber et al., 2007), because of the absence of external electrodes. In particular, for stage N2 and N3, scoring was based on the preponderance of spindles, K-complexes and occasional slow waves in N2, and more continuous slow waves in N3. We included at least 60 min of stage N2 and N3 in the first part of the night after sleep onset (Table 1 for details regarding time of selected recordings and medication for each patient). For each patient, we obtained on average 76.43 min (range 60–112) of sleep, when spindles are most visible.

Based on the clinical reports and on visual inspection, channels exhibiting epileptic activity were excluded. On average, the percentage of excluded channels was 8.90% (range 2.50–23.75%), mostly over the postcentral areas (12 channels), the middle temporal region (10 channels), and the supramarginal gyrus (9 channels). The number of electrodes included in the analysis per patient was on average 78.75 (range 57–93). The signal of the these channels was re-referenced to the common average (Canolty et al., 2006; Hermes et al., 2015). Recordings were then filtered at 0.5 Hz (high-pass filter) and at 50 Hz (low-pass filter) and subsequently resampled to 256 Hz.

Analyses were carried out in Python 3.4 with numpy (1.9.2), scipy (0.16), and vispy (0.5). The code for the analysis can be requested from the corresponding author.

Electrode locations

Electrode positions were picked manually from the post-surgery cortical tomography (CT) scans and realigned to the pre-surgery magnetic resonance imaging (MRI) using SPM (as described in detail in Dykstra et al. (2012)). Cortical surfaces were computed with FreeSurfer (Dale et al., 1999; Fischl et al., 1999). To account for misalignment between the MRI and CT and distortion of the brain structure due to the craniotomy, the locations of the grid electrodes were projected onto the cortical surface (Fig. 1).

The coverage across all subjects shown in the bottom panel of Fig. 1 was generated by projecting a sphere with a 10 mm Gaussian window for each electrode onto the subject-specific anatomical space and realigning this subject-specific map onto the average brain surface using surface-based normalization (Fischl et al., 1999), after flipping a

Table 1
Patients' characteristics.

ID	Sex	Age	Hemi	Onset	Medications	Diagnosis	Resection	Start time	Duration
S1	M	43	R	~30	CLZ, LCS, LTG, ZNS	M.T.S.	O.F./AntTemp	23:44:38	67.5
S2	F	46	R	15	CLZ	C.D.	AntTemp	01:54:30	60.5
S3	M	29	L	18	LTG, LEV	C.D./Het.	S.T./AntTemp	00:35:22	98.5
S4	M	25	L	16	LTG, LEV, PNT, TPR	Unclear	MedTemp	00:06:14	67.0
S5	F	21	L	Unknown	LCS, LTG	Post-infarct	Temporal	00:53:11	61.5
S6	M	45	R	15	PNT	Unknown	AntTemp	01:40:42	60.0
S7	M	37	R	18	CRB, CLZ, LEV	Unknown	Prefrontal	21:16:19	112.0
S8	M	47	R	38	None	Unknown	None	23:02:21	81.5

Description of the patients' profiles. Patient population was heterogeneous in terms of age, epilepsy form, age of onset, cortical area, suggesting that no single particular aspect biased the findings. Start time of the sleep period is given in the format hour:minute:second and the duration is in minutes. Abbreviations for the medications taken during the recordings are CRB: Carbamazepine, CLZ: Clonazepam, LCS: Lacosamide, LEV: Levetiracetam, LTG: Lamotrigine, PNT: Phenytoin, TPR: Topiramate, ZNS: Zonisamide. Abbreviations for the diagnosis are C.D.: cortical dysplasia, Het.: heterotopia, M.T.S.: mesial temporal sclerosis. Abbreviations for the resection are AntTemp: anterior temporal, MedTemp: medial temporal, O.F.: orbitofrontal, S.T.: subpial transection.

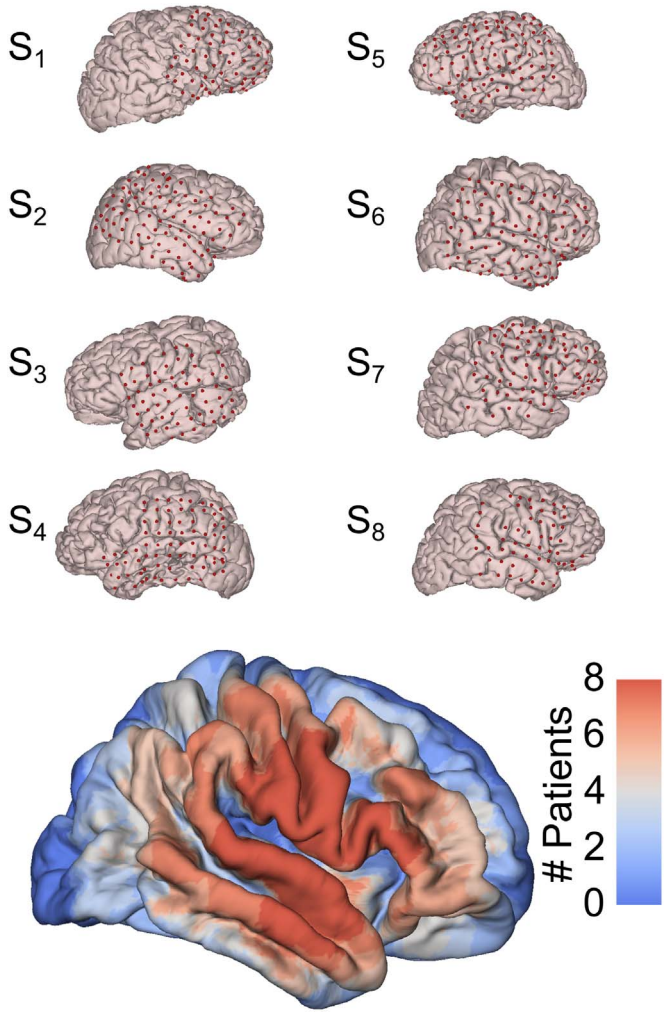

Fig. 1. Localization of electrodes for each individual subject and coverage map on the average brain surface. Red dots indicate the location of the electrodes onto the pial surface. The grids of each of the eight patients included in the study covered almost all the lateral regions of the cortex. The location of each electrode was projected onto the subject-specific anatomical space and then realigned using surface-based normalization (Fischl et al., 1999), after flipping left-hemisphere grid to the right anatomical space.

left-hemisphere grid to the right anatomical space.

For the statistical analysis, each electrode was assigned to one of the 58 unilateral cortical regions from the Connectome atlas (Cammoun et al., 2012; Daducci et al., 2012), a more refined parcellation scheme of the Desikan-Killiany atlas (Desikan et al., 2006). The parcellation was computed in FreeSurfer based on the Connectome classifier atlas available at https://github.com/LTS5/cmp/tree/master/cmp/data/colortableandgcs/myatlasgcs. Because of this improved parcellation, a single label of the Desikan-Killiany atlas might refer to multiple cortical regions of the Connectome atlas. The labels of the cortical regions used in this manuscript follow that atlas' nomenclature. An electrode was assigned to the closest cortical region in Euclidean distance.

Spindle detection

Spindles were detected on each electrode independently, using previously reported methods with stringent criteria (Ferrarelli et al., 2007; Nir et al., 2011). The raw signal was filtered between 9 and 16 Hz and the instantaneous amplitude was calculated by taking the envelope of the analytic representation, whose imaginary part contains the Hilbert transform. A spindle was detected when it fulfilled these criteria: 1) The amplitude had to be above a threshold for detection (set at 3 times the S.D. of the envelope of the analytic representation calculated for each subject and electrode). 2) The beginning and end of the spindle were defined by a threshold for selection (set at the S.D.). 3) Spindle duration had to be between 0.5 and 2 s. 4) The peak of the power spectrum from the raw signal over the spindle interval had to lie between 9 and 16 Hz. The last criterion was introduced to remove transient events with a broadband profile (Andrillon et al., 2011; De Gennaro and Ferrara, 2003).

Spindle characteristics

To investigate whether spindle characteristics are uniform over the cortex, we tested the hypothesis that spindle density, the mean peak in the power spectrum of the spindle frequency band, the mean spindle amplitude, and the mean spindle duration have different values or not depending on the cortical location in which they are observed. Spindle density, in spindles per minute, was computed by dividing the number of spindles by the duration of the sleep period. For each spindle, we computed the peak in the power spectrum, whose frequency resolution depended on the duration of each spindle, was computed for each spindle and the values of all the spindles of the same electrode were averaged into one value per electrode. The duration and the maximum amplitude were computed for each spindle and averaged over each electrode.

Statistical testing

The central research question was whether the spindle characteristics defined above vary across different brain regions. To test this, we assessed whether some brain regions have significantly higher or significantly lower values than the average of the other regions, where the estimated value (with its variance) for each region was estimated from the electrodes in that region. The positioning of the electrodes for each patient was decided uniquely based on clinical criteria and therefore the coverage of the grid differed across patients. Furthermore, the ability to reduce the influence of outliers is central to obtaining a robust estimate of the underlying phenomenon of interest. These fundamental problems limit the application of statistical tools, such as analysis of variance (ANOVA), that expect a fixed number of degrees of freedom for each brain region and patient and that are sensitive to aberrant values.

A powerful and flexible framework to deal with unequal number of electrodes across patients and with potential outliers is provided by a linear mixed-effects regression model (LMEM) (Pinheiro and Bates, 2000). According to the LMEM theory, the expected value of interest (such as spindle density) of one brain region can be calculated from the values of the single electrodes in that region, based on the assumption that each electrode value is a linear combination of the expected value for the brain region, an offset specific to the patient, and an error term specific to the electrode. The observed value y at electrode position i is: $y_i = X_i\beta + Zb_i + \varepsilon_i$, where X is the matrix that describes to which brain region the electrode i belongs to, Z describes to which patient the electrode i belongs to and the value b_i is the random-effects value for each patient, such that $b_i \sim N(0, \Psi)$ with Ψ being the covariance matrix of the random effects. The term b_i represents the intercept for each subject and, therefore, accounts for the inter-individual variability that has been reported for some of the measures under investigation (De Gennaro and Ferrara, 2003; Werth et al., 1997). The regression coefficient can be estimated using Restricted Maximum Likelihood (ReML) and the standard error of the ReML estimates is used to compute the z-value, which can then be summarized as p-values by applying a Wald test. We report the estimates computed from ReML. Analysis was conducted in R 3.2 (R Development Core Team, 2010), using the package lme4 (Bates et al., 2015). An omnibus test was run to assess whether there were differences between brain regions and specific post-hoc tests quantified the differences between selected brain regions, after false discovery rate (FDR) correction was applied to

account for multiple comparisons across brain regions (Benjamini and Hochberg, 1995). The combination of LMEM and surface-based realignment has been shown to be highly accurate and sensitive to the underlying effect of interest (Kadipasaoglu et al., 2014; Mak-McCully et al., 2015).

Spindle co-occurrence

To measure the spatial extent of spindle activity, we quantified the number of channels that had co-occurring spindles at each time point when at least one spindle was present. This measure returns the histogram of the number of time points with co-occurring spindles, based on the number of channels that had co-occurring spindles. The histogram values were then converted to percentage time spent, where 100 represents the total amount of time when at least one spindle was observed in any channel.

We first investigated whether there were differences in the spindle characteristics between the most isolated and the most widespread spindles. For each participants, we took the mean of peak frequency, amplitude, and duration of the 10% most isolated spindles and of the 10% most widespread spindles. These spindle characteristics were compared using a paired *t*-test.

We tested the hypothesis that the co-occurrence of spindles varies across brain regions, with some regions more involved in the co-occurrence of spindles. For each time point when a spindle was present in a channel of interest, we measured how many other channels had co-occurring spindles. This approach creates a distribution of the number of time points based on the number of channels with co-occurring spindles. Because the distribution were not normally distributed (see Results), we took the median of the distribution values, which indicates the average number of spindles that co-occur with a specific spindle in that channel of interest. As above, we applied LMEM to test if and which regions had significantly higher or lower estimates of average number of channels with co-occurring spindles as compared to the average. The values were visualized onto the average brain by projecting the estimated values at each brain region to the template average brain.

Spindle propagation

In addition to the co-occurrence of spindles, which tests for the simultaneity of these events, we tested whether there exists a preferential sequence of spindles between brain regions. Each overlapping spindle pair was classified as one leading spindle and one lagging spindle, based on their start times. For each pair of brain regions, we computed the log-ratio of leading-to-lagging spindles, which results in an antisymmetric matrix. As some of the region pairs did not have any overlapping spindles, the ratio between those regions was not considered in the subsequent analysis.

To assess whether some regions were more likely to have leading or lagging spindles, we performed a permutation test, a type of non-parametric statistical test. The advantages of this test are that it does not assume that the data is normally distributed and that the randomization procedure takes into account some characteristics of the data, e.g. some cells of the leading/lagging matrix are empty (region pairs without overlapping spindles) and there might be a different number of spindle pairs across regions. To compute this test, we averaged the matrix of the ratio values to obtain a mean value for each brain region and we tested whether any of these average ratios were significantly different from what we would expect by chance. The null hypothesis is therefore that the ratio of leading-to-lagging spindles at each region pair was not different from that observed from a binomial distribution with probability of 0.5 and the same number of total spindle pairs. In this way, we generated 10'000 surrogate antisymmetric matrices where each cell contained the log-ratio obtained from the binomial distribution and took the mean value for each brain region. This procedure results in a distribution, for each brain region, of the mean ratio values under the null distribution. We then compared the observed values against this distribution to obtain two-tailed region-specific *p*-values, which were subsequently FDR corrected.

Results

Electrode locations

The electrode locations varied across patients due to the individual clinical profiles. Five patients had coverage of the right hemisphere and three patients had coverage over the left hemisphere (Table 1). Coverage was highest over the lateral posterior prefrontal cortices and the anterior temporal cortices based on the projected activity of each electrode onto the cortical surface using a Gaussian window with a 10 mm standard deviation (Fig. 1). The medial surfaces and the most caudal occipital region did not have substantial coverage. Thirty-eight out of 58 unilateral cortical regions, as defined by the parcellation atlas (Cammoun et al., 2012; Daducci et al., 2012), were included in the subsequent analyses.

Spindle characteristics

Spindles were observed over almost all the cortical areas investigated in this study (Fig. 2). The highest number of spindles per minute was concentrated over lateral prefrontal and subfrontal regions, while temporal regions had a low spindle count (Fig. 3 A). To assess statistically if there were differences in the spindle parameters between brain regions, we applied LMEM to the values measured at each electrode. Based on the brain reconstruction, each electrode was assigned a label indicating to which region the electrode belonged. First, we quantified the number of spindles per minute at each electrode. An LMEM, which is designed to handle missing data, control for unequal degrees of freedom due to differences in coverage, and minimize the influence of outliers, was computed to test the hypothesis that the number of spindles is different between brain regions.

The estimated average value for the number of spindles per minute was 0.919. Frontal regions had a significantly higher spindle density (rostral middle frontal regions, anterior part: 2.278 spindles/min, p=0.004, medial part: 1.349 spindles/min, p=0.004, posterior part: 1.210 spindles/min, p=0.012; pars triangularis: 1.239 spindles/min, p=0.019; caudal middle frontal region: 1.194 spindles/min, p=0.043) than the estimated average value, in addition to the superior part of post-central gyrus (1.296 spindles/min, p=0.009). In contrast, regions in temporal cortex, in addition to the lower part of the post-central

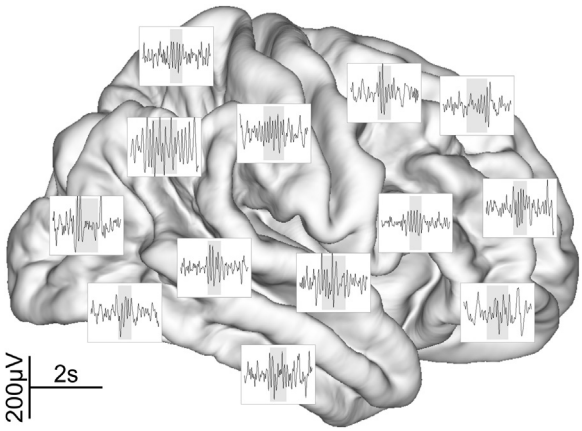

Fig. 2. Spindles were present in all the recorded cortical regions. Each inset shows a 2 s time window with the highlighted spindles from different subjects, where the location in the plot indicates the approximate position of the electrode where the spindle was detected.

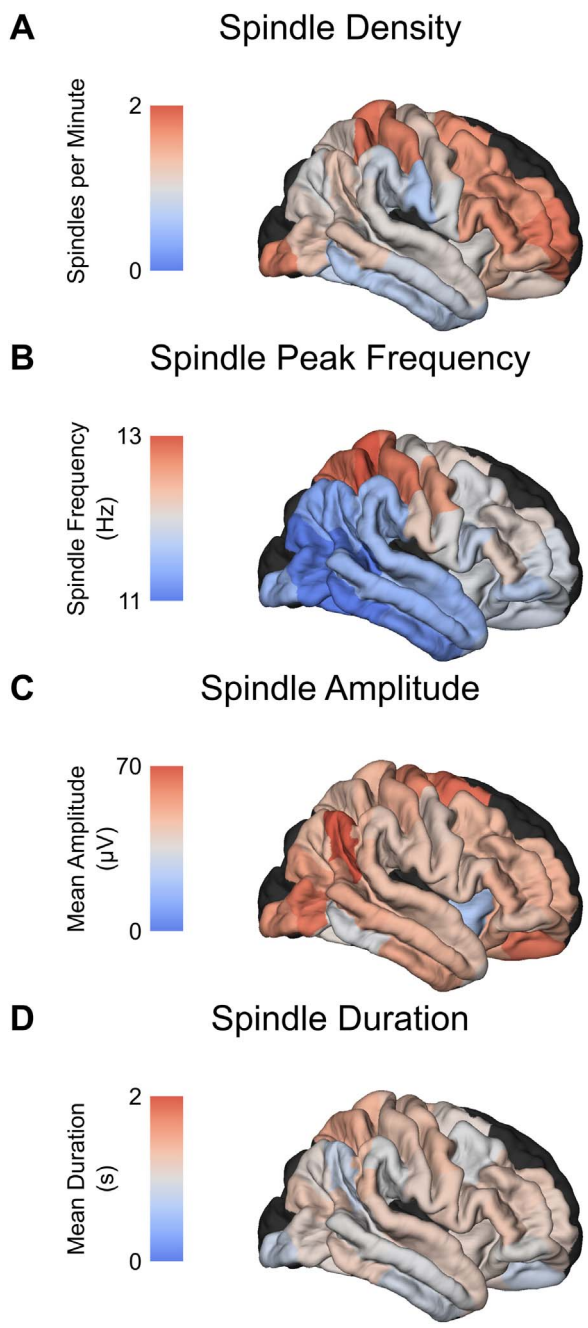

Fig. 3. Spindle density and peak frequency vary with cortical location while amplitude and duration do not. The number of spindles per minute was significantly higher in the prefrontal cortex and superior parietal region, as compared to the other regions. Spindle frequency was highest over superior parietal region and progressively decreases towards prefrontal regions, in agreement with the putative sources of fast and slow spindles observed on the scalp. Intriguingly, the slowest spindles were observed in the inferior temporal and the inferior parietal cortices. Other spindle properties, such as amplitude and duration, on the other hand, remain constant throughout the cortex.

gyrus (0.563 spindles/min, p=0.035; 0.504 spindles/min, p=0.007), had significant lower spindle density (inferior temporal cortex: 0.577 spindles/min, p=0.012; middle temporal cortex: 0.671 spindles/min, p=0.007).

There was a remarkable variability in the peak frequency of the spindle across brain regions, measured from the mean of the peak in the power spectrum of the spindle frequency band, as compared to the estimated mean value of 11.730 Hz (Fig. 3B). The lowest spindle frequency, indicating the slowest spindles, was observed over temporal regions, with lower values in more inferior regions (fusiform gyrus: 10.616 Hz, p=0.016; bank of the superior temporal sulcus: 10.620 Hz, $p < 0.001$; inferior temporal gyrus: 10.791 Hz and 11.165 Hz, $p < 0.001$; middle temporal gyrus: 11.438 Hz, p=0.010; superior temporal gyrus: 11.444 Hz, p=0.033) and inferior parietal regions (inferior parietal cortex: 10.885 Hz, p=0.016). The higher spindle frequency was found to follow the frontal-to-parietal gradient that is commonly reported in the scalp EEG, whereby the fastest spindles are located in the superior parietal cortex (13.166 Hz, $p < 0.001$ and 12.825 Hz, p=0.016), and become slower in more inferior and frontal regions (post-central gyrus: 12.784 Hz, $p < 0.001$, 12.341 Hz, p=0.002, 12.179 Hz, p=0.016; pre-central gyrus: 12.541 Hz and 12.514 Hz, $p < 0.001$; pars triangularis: 12.141 Hz, p=0.016; rostral middle frontal cortex: 12.084 Hz, p=0.016).

There was some variation between brain regions in terms of mean spindle amplitude, measured from the peak of the envelope of the analytic representation of the bandpass-filtered recordings, with an average of 51.424 μV (Fig. 3 C). Regions with significantly higher mean amplitude were the medial orbitofrontal cortex (96.539 μV, p=0.007, 95.238 μV, p=0.008) and the inferior parietal cortex (71.731 μV, p=0.007). Only the inferior part of the post-central gyrus and the inferior temporal regions had significantly lower mean spindle amplitude (respectively, 36.888 μV, p=0.016 and 34.206 μV, p=0.036). In spite of the large range in terms of estimated values, only few regions were significantly different from the average, probably due to the variability across patients and electrodes. A source of variability between electrodes is the distance between the electrodes and the brain surface, which might have affected the absolute measure of amplitude at the single-channel level. However, the variability in absolute amplitude across channels is not expected to affect the other measures as spindle detection relied on thresholds based on relative amplitude, therefore accounting for much of the underlying variability.

Very little variation across brain areas was observed for the mean spindle duration, where only one subregion of the precentral gyrus had a significantly longer duration than the estimated average value of 1.278 s (estimated mean duration for the precentral subregion was 1.401 s, $p < 0.001$; Fig. 3 D).

Spindle co-occurrence

The spatial extent of the sleep spindle was investigated by quantifying the number of channels with co-occurring spindles at any given time (Fig. 4A). For each subject, we then created a histogram of the time points based on the number of channels with co-occurring spindles (Fig. 4 B) and expressed the values as percentage of the total time when at least one spindle was detected anywhere. The subject-specific histograms reveal, overall, that spindles tend to co-occur over a very limited number of channels; in fact, the large majority was limited to no more than 3 channels. However, there were short periods in which spindles occurred over multiple channels, up to 20, at the same time.

We then tested whether the spindle characteristics of interest different between the most isolated and the most widespread spindles. The 10% most isolated spindles and the 10% most widespread spindles did not differ in frequency (mean isolated spindles 11.885 Hz, mean widespread spindles: 11.897 Hz, paired $t(7)=-0.121$, p-value=0.907), amplitude (mean isolated spindles 51.923 μV, mean widespread spindles: 51.453 μV, paired $t(7)=0.326$, p-value=0.754), or duration (mean isolated spindles 1.559 s, mean widespread spindles: 1.332 s, paired $t(7)=1.559$, p-value=0.163).

To test the hypothesis that there is an underlying spatial dependence in the likelihood of observing spindle co-occurrence, we employed, as above, LMEMs, which are designed to account for the contribution of inter-individual offsets to the number of co-occurring spindles in multiple brain regions. We computed a distribution of the number of channels with co-occurring spindles when a spindle was present in the channel of interest. The distribution for each channel

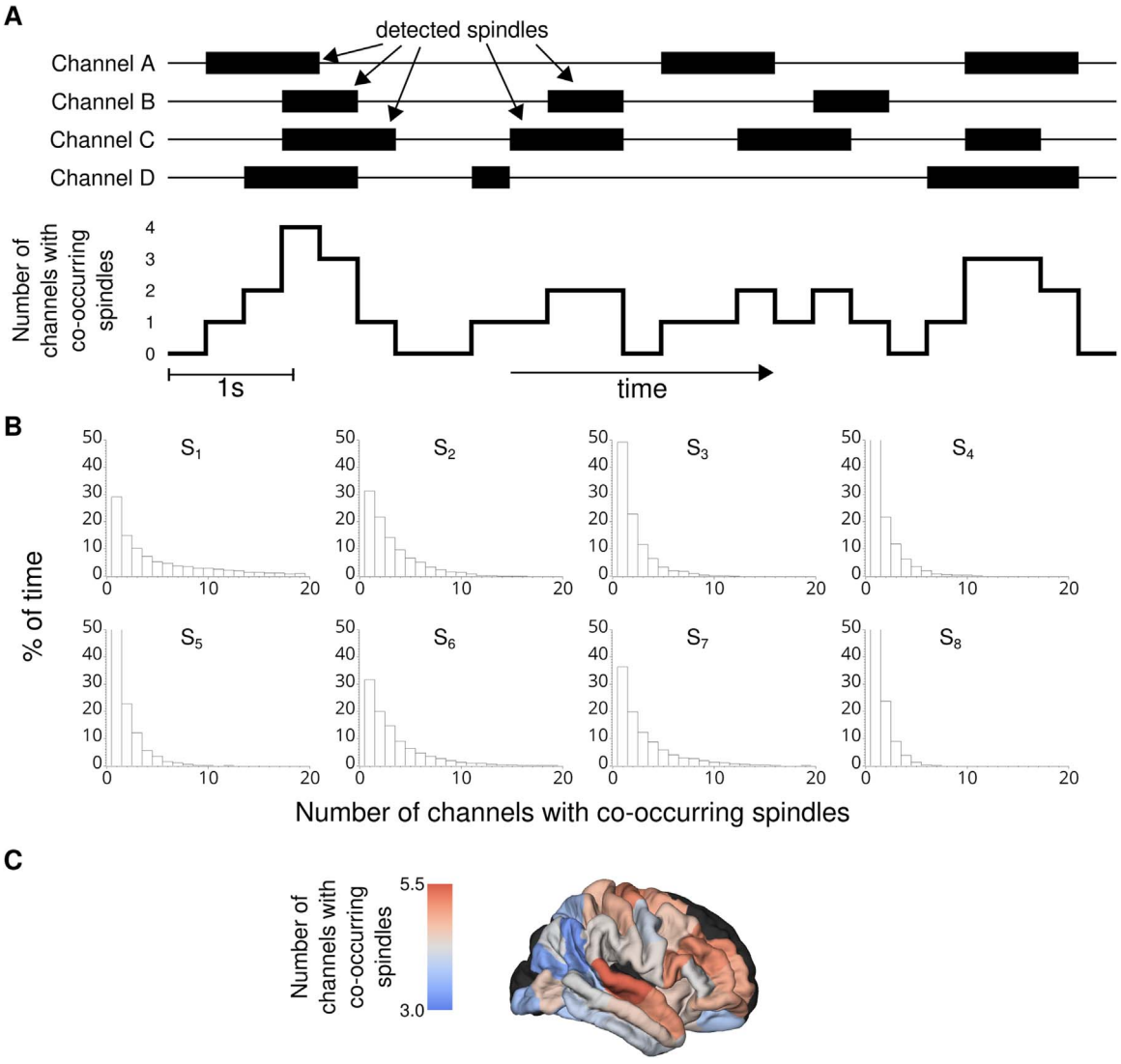

Fig. 4. The number of channels with co-occurring spindles is small, but there is variability in time and space. (A) The analysis procedure is described in this schematic representation. We computed the number of channels with co-occurring spindles at every time point, which was used to create a histogram of its distribution. (B) The histograms of the number of channels with co-occurring spindles for each subject show that most spindles are only present in one or a few channels at any given time. However, there are periods in which spindles are present over up to 10–15 channels simultaneously. The differences across subjects are likely affected by the electrode location over different cortical regions. (C) Spindles present over the lateral prefrontal cortex and superior temporal gyrus tend to co-occur with a larger number of spindles in other channels, as compared to spindles in the parietal region. For each channel, we computed a distribution of the number of other channels with co-occurring spindles, if a spindle was present in the channel of interest. We used LMEM on the median of the distribution at each channel to take into account the variability across subjects.

and subject was summarized by its median, because we observed that the distribution was not normally distributed (Fig. 4B), and entered in the LMEM to test whether there are regions that have a higher or lower number of channels with co-occurring spindles. We found that the superior temporal and the rostral middle frontal cortices were more likely to have co-occurring spindles than the averaged estimated value of 4.318 (rostral middle frontal region: 5.107, p=0.029; superior temporal regions: 5.398 $p < 0.004$, 5.044 p=0.029; Fig. 4C). Only one subregion of the medial orbitofrontal cortex had a significantly lower number of channels with co-occurring spindles (0.690, p=0.009).

Spindle propagation

The preferential direction of spindle propagation was assessed by classifying each spindle pair of groups of co-occurring spindles as one leading and one lagging spindle (Fig. 5 A). Each pair of regions was therefore characterized by a ratio in the total number of leading and lagging spindles between those two regions. Fig. 5 B shows the ratio between all the region pairs in the form of an antisymmetric matrix, and Table 2 summarizes the region pairs where the ratio was particularly skewed (i.e. ratio was higher than 2:1, with at least 100 spindle pairs). Two major propagation pathways were observed: from the temporal cortex to the orbitofrontal cortex and from the caudal frontal cortex to the orbitofrontal cortex.

To determine whether this relationship was statistically significant, we obtained, for each brain region, the average value of the ratio between leading and lagging spindles. The null hypothesis was tested using a non-parametric distribution of surrogate values, computed by keeping the same number of spindle pairs between regions and by using a probability of 0.5. The observed values were compared against the non-parametric distribution to obtain a two-tailed p-value for each region, which were subsequently FDR corrected. Regions more likely to have leading spindles included the superior temporal gyrus including surrounding areas (superior temporal region: estimated ratios 1.246:1 and 1.176:1, $p < 0.001$; middle temporal gyrus 1.091:1, p=0.003; insula 1.179:1, p=0.005) and the superior frontal regions including surrounding areas (precentral area 1.365:1, $p < 0.001$; superior frontal regions 1.249:1, p=0.001; superior parietal 1.242:1, p=0.008; post-

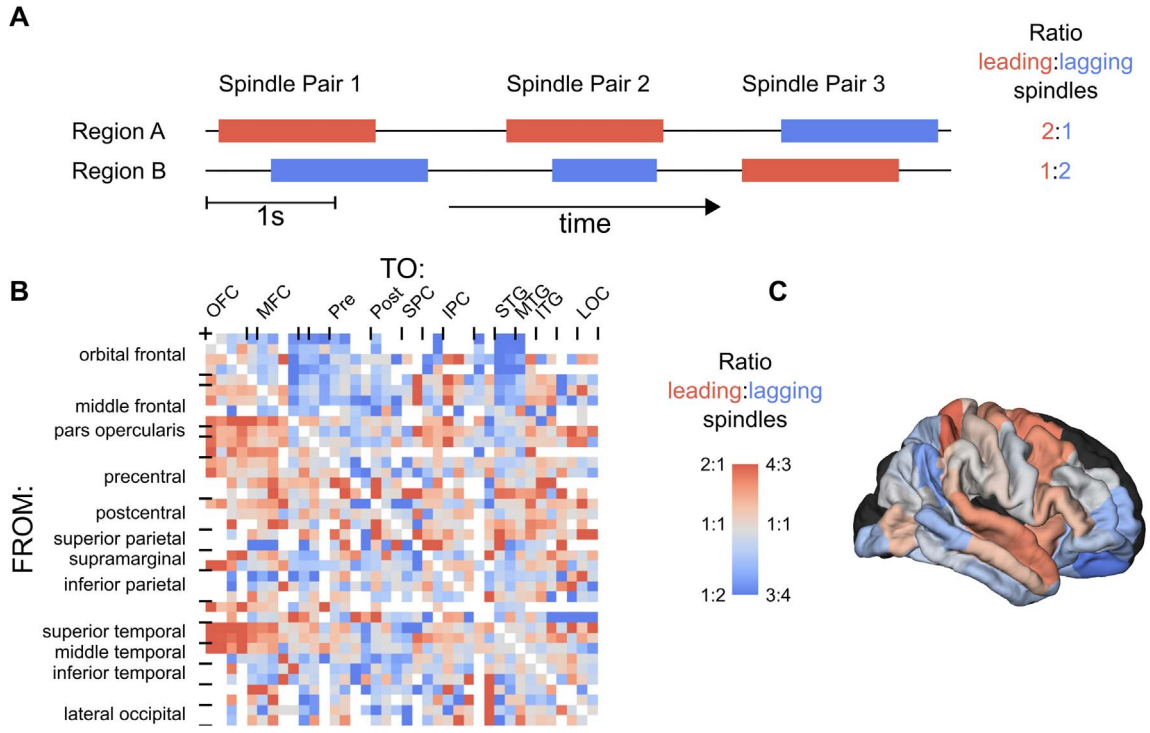

Fig. 5. Spindles have a bias to propagate from the superior frontal and temporal regions towards the orbitofrontal cortex. (A) Each pair of regions A and B was assigned a ratio depending on whether spindles in region A were leading or lagging spindles in region B. In this example, two spindles occur first in region A and only one occurs first in region B, so that the ratio becomes 2:1. (B) This measure was computed for each pair of regions, to create an antisymmetric matrix indicating the ratio of spindle directionality between brain regions. We found that the spindles in the superior frontal and temporal regions tend to precede spindles in the orbitofrontal cortex, with a ratio larger than 2:1 (see Table 2 for detailed results). (C) The ratio of leading-to-lagging spindles was averaged for each brain regions, showing the location of the regions which were more likely to have leading spindles and those which were more likely to have lagging spindles.

Table 2
Brain regions where spindle propagation was most pronounced.

From	To	# Spindle pairs	Ratio
superior temporal (2)	medial orbitofrontal (1)	116	3.640:1
middle temporal (2)	lateral orbitofrontal (2)	320	3.000:1
superior temporal (1)	medial orbitofrontal (2)	114	2.931:1
insula (2)	lateral orbitofrontal (2)	150	2.846:1
pars triangularis (1)	inferior parietal (1)	110	2.793:1
superior temporal (2)	lateral orbitofrontal (2)	460	2.622:1
superior temporal (1)	lateral orbitofrontal (1)	260	2.514:1
pars orbitalis (1)	inferior parietal (1)	109	2.406:1
superior temporal (1)	lateral orbitofrontal (2)	365	2.380:1
caudal middle frontal (1)	lateral orbitofrontal (1)	718	2.220:1
precentral (3)	precentral (1)	106	2.118:1
rostral middle frontal (2)	inferior parietal (1)	146	2.106:1
caudal middle frontal (1)	lateral orbitofrontal (2)	1329	2.062:1
caudal middle frontal (1)	pars orbitalis (1)	1645	2.013:1

Pairs of brain regions with a high ratio of leading-to-lagging spindles (i.e. ratio higher than 2:1 and at least 100 spindle pairs) for all the spindles across subjects. The number in brackets is used to differentiate the subregions of the Desikan-Killiany atlas.

central gyrus 1.226:1, p=0.046; caudal middle frontal gyrus 1.206:1, $p < 0.001$; pars opercularis 1.121:1, p=0.001; pars triangularis 1.086:1, p=0.041). The orbitofrontal and the rostral middle prefrontal cortices, on the other hand, were areas with more lagging than leading spindles (medial orbitofrontal regions 1:1.787 and 1:1.409, $p < 0.001$; lateral orbitofrontal region 1:1.438, $p < 0.001$; rostral middle frontal regions 1:1.382, p=0.007, 1:1.144, p=0.004), in addition to one subregion in the middle temporal cortex (1:1.115, p=0.017) and one subregion in the inferior parietal area (1:1.243, p=0.001).

4. Discussion

Using intracranial recordings placed directly on the pial surface in humans, we have found that spindles are a heterogeneous graphoelement, whose local characteristics are affected by the underlying cortical regions. Spindles per minute were significantly higher in prefrontal regions and their fundamental frequency band varies from fastest spindles over parietal regions, to slowest spindles in the temporal cortices, while prefrontal spindles were of intermediate frequency.

The spatial extent of spindles varied substantially, although the distribution was strongly skewed towards highly isolated spindles. Only a subset of spindles occur over widespread areas, especially those involving the lateral prefrontal cortex and the superior temporal gyrus. There was a subtle but significant preference in the propagation of spindles from the superior prefrontal regions and the temporal cortices towards the orbitofrontal cortex. Overall, these findings suggest that spindles are a local event. However, this does not imply that spindle properties are disorganized, as their local characteristics and patterns of co-occurrence and propagation follow a complex brain-wide spatial organization revealed by ECoG.

Local characteristics

Our results show that the sleep spindle is an event that occurs throughout the brain and whose properties are strongly affected by the cortical regions from where it arises. Spindles were detected in all the cortical regions under investigation, which represent large portions of the lateral brain surface, including the temporal cortex and the occipital cortex (Fig. 2 and Fig. 3A). These observations build on the increasing evidence in favor of the existence of temporal spindles (Clemens et al., 2011; Frauscher et al., 2015; Malow et al., 1999; Sarasso et al., 2014), although some studies, also using ECoG, found no narrow-band spindle activity in the inferior temporal cortex (Nakabayashi et al., 2001; Nakamura et al., 2003; Peter-Derex et al., 2012). Interestingly, we observed a very low spindle density in this region.

Although spindles were observed in all the brain areas under investigation, their properties vary depending on the spatial location. The highest concentration of spindles was observed in the prefrontal cortex and the superior parietal cortex, in agreement with studies that employed source-reconstruction analysis from scalp EEG and MEG (Anderer et al., 2001; Gumenyuk et al., 2009; Manshanden et al., 2002; Siclari et al., 2014; Urakami, 2008). In contrast to some of these studies, however, our recordings indicate that spindles are present in multiple locations instead of a few focal deep sources. This might result from the known difficulties of performing cortical localization with EEG/MEG for highly distributed sources (Wennberg and Cheyne, 2013).

The peak frequency in the spindle band was the characteristic that was most dependent on the underlying cortical location. We observed two major gradients of spindle frequency: the first spanning from the fastest spindles in superior parietal regions to slower spindles in the prefrontal cortex, and the second spanning from the slowest spindles in the inferior temporal gyrus towards slightly faster spindles in more superior regions. The first gradient has been well reported in the scalp literature, with a major distinction drawn between fast/parietal and slow/frontal spindles (Mölle et al., 2011, 2002; Werth et al., 1997), indicating a strong agreement between the EEG literature in healthy participants and the findings in the current ECoG study in patients with epilepsy. Intriguingly, we find that the transition between fast and slow spindles seems to follow a linear pattern over the parietal and frontal regions, in agreement with previous work (Peter-Derex et al., 2012), instead of a clear dichotomy between fast and slow spindles (Andrillon et al., 2011; Ayoub et al., 2013).

Other characteristics, such as spindle amplitude and spindle duration, were, on the other hand, rather constant across the cortex. An intriguing explanation for the spatial variability in spindle frequency but not in these other characteristics might be related to the effect of natural resonance frequencies. These are thought to be dependent on the anatomical structure of the thalamocortical modules (Rosanova et al., 2009), in particular that of the white-matter tracts that have been shown to affect the characteristics of the sleep waves (Piantoni et al., 2013).

Synchronization of spindles

The observation that the spindle is a local event that is finely organized throughout the cortex is confirmed by the findings on the synchronization of spindles over multiple cortical regions, in terms of co-occurrence and propagation. Most spindles co-occur over restricted cortical areas, often inside the same brain region, in agreement with previous iEEG findings (Johnson et al., 2012; Nir et al., 2011; Nobili et al., 2012). However, we found temporal and spatial exceptions to this statement: during relatively short periods, spindles might co-occur over large areas, and they were more likely to be widespread if they involved the lateral prefrontal and superior temporal cortex (Fig. 4). These differences did not depend on any other characteristics apart from the spatial location, as the most isolated spindles and the most widespread spindles did not differ in peak frequency, amplitude or duration. Furthermore, spindles in multiple locations show a preference for propagation from the superior frontal, parietal, and temporal cortices towards the orbitofrontal cortex, in accordance with scalp EEG work (O'Reilly and Nielsen, 2014).

Taken together, these results support the notion that, while spindles are a local phenomenon, there exists an organization of local and synchronization properties at the broad cortical level. This interpretation suggests the presence of an underlying mechanism that orchestrates spindle activity. Anatomical, electrophysiological, and computational work overwhelmingly identifies the thalamus as the putative conductor (Bazhenov et al., 2002; Steriade et al., 1993a). According to this interpretation, the relative contribution of specific thalamocortical pathways to spindle activity affects its synchronization properties, whereby focal spindles may be generated by the spatially restricted core thalamocortical system and widespread spindles may reflect the distributed matrix system (Bonjean et al., 2012; Piantoni et al., 2016). Previously, we were able to assign spindles to either of these two thalamocortical systems by observing their spatial characteristics and presence in either MEG or EEG, simultaneously recorded (Dehghani et al., 2011a; Dehghani et al., 2010b). In this light, the current finding that the spatial extent of spindles varies between brain areas is in agreement with the observations that the distribution of the matrix and core pathways might not be homogeneous throughout the cortex (Clascá et al., 2012; Jones, 2001; Piantoni et al., 2016).

A comparison between spindles and K-complexes might shed light on the underlying similarities and differences of these two characteristic graphoelements of NREM sleep. Similar to what we show here for spindles, K-complexes can arise in any cortical area, but at different rates, and, like spindles, they can be isolated to a single electrode, or they can spread to variable extents, and in variable directions (Mak-McCully et al., 2015). Although K-complexes and spindles are often temporally linked and their generators overlap spatially, we find a major difference between these two graphoelements in their preferred direction of propagation. While K-complexes and slow waves have a subtle but statistically significant bias to propagate from frontal to posterior regions (Mak-McCully et al., 2015; Massimini et al., 2004), spindles had a largely opposite preferred direction of propagation. This difference might be the result of the underlying cortical generators: while spindles arise in thalamocortical networks, K-complexes and slow waves are thought to be triggered by cortical events (Cash et al., 2009; Steriade et al., 1993b). Further studies, including modeling work, are needed to define a common framework in which thalamocortical and corticocortical connections facilitate the co-occurrence and propagation of spindles and K-complexes over cortical regions.

Because spindles may play a central role in the local regulation of cortical plasticity (Rosanova and Ulrich, 2005), their ubiquity might indicate that a common, yet highly spatially differentiated, mechanism takes place throughout the cortex. This mechanism is thought to represent the physiological correlate of memory consolidation (Diekelmann and Born, 2010). While memories are widely encoded throughout the brain, the interaction between temporal and prefrontal regions is of particular relevance (Simons and Spiers, 2003). This pattern reflects the topographical map of spindle co-occurrence observed in this study: spindles are in general more likely to be limited to a single cortical region, but those in the superior temporal and lateral prefrontal areas have a more widespread extent.

Limitations

The wider availability of intracranial recordings in patients with epilepsy has resulted in a growing number of studies investigating sleep rhythms with invasive techniques (Andrillon et al., 2011; Frauscher et al., 2015; Nir et al., 2011; Nobili et al., 2012; Sarasso et al., 2014; Valderrama et al., 2012). This unique opportunity comes with the concern that findings obtained in this particular population might not generalize to a control population (Beenhakker and Huguenard, 2009), especially because of the effects of anti-epileptic drugs (Bazil, 2003). This concern is allayed by the increasing concordance between findings in healthy controls and findings in patients with epilepsy as the latter become more studied (Lachaux et al., 2003). Results of the current work parallel previous findings in the literature in healthy participants, such as the prevalence of spindle activity over frontal and superior parietal regions, supported by source-reconstruction studies (Siclari et al., 2014), and by the gradient in spindle frequency between faster parietal spindles and slower posterior spindles (Anderer et al., 2001; Gumenyuk et al., 2009). Thanks to the ability to record directly from the pial surfaces, we were able to integrate these observations with novel findings, especially in regions that are more difficult to investigate using non-invasive approaches, such as the temporal cortex.

Unfortunately, we were not able to perform a direct comparison between spindles observed in intracranial and scalp recordings (Andrillon et al., 2011; Dehghani et al., 2011b; Frauscher et al., 2015) as the placement of the ECoG grid requires a craniotomy, which distorts the scalp EEG due to field inhomogeneities and fluid accumulation and carries a risk of infection (Cobb et al., 1979; Csercsa et al., 2010).

Conclusions

Spindles are present in all the areas under investigation, but are not a uniform phenomenon. The local characteristics follow a complex pattern, whereby density and peak frequency were specific to the underlying cortical regions. While mostly isolated events, spindles might nevertheless occur over large regions for brief periods, especially when involving the prefrontal and temporal cortices. Overall, these results characterize the sleep spindle as a complex phenomenon, whose region-specific properties reveal an overarching brain-wide organization. The interplay between local and widespread characteristics may be necessary to provide a flexible framework for the many functions attributed to the spindles.

Conflict of interest

The authors have indicated no financial conflicts of interest with the work in this manuscript.

Acknowledgments

This work was supported by BIAL Foundation (220/12) to GP; Office of Naval Research (N00014-13-1-0672); and National Institute of Health (R01 EB009282 and MH099645). We thank Jason Naftulin and Mia Borzello for their support and assistance in gathering data; Jean-Baptiste Eichenlaub, Alice Lam, and Sujith Vijayan for helpful comments on the manuscript; the staff of the Epilepsy Monitoring Unit at MGH for technical assistance; and the patients for their participation.

References

Achermann, P., Borbély, A.A., 1998. Coherence analysis of the human sleep electroencephalogram. Neuroscience 85, 1195–1208.
Anderer, P., Klösch, G., Gruber, G., Trenker, E., Pascual-Marqui, R.D., Zeitlhofer, J., Barbanoj, M.J., Rappelsberger, P., Saletu, B., 2001. Low-resolution brain electromagnetic tomography revealed simultaneously active frontal and parietal sleep spindle sources in the human cortex. Neuroscience 103, 581–592.
Andrade, K.C., Spoormaker, V.I., Dresler, M., Wehrle, R., Holsboer, F., Sämann, P.G., Czisch, M., 2011. Sleep spindles and hippocampal functional connectivity in human NREM sleep. J. Neurosci. 31, 10331–10339.
Andrillon, T., Nir, Y., Staba, R.J., Ferrarelli, F., Cirelli, C., Tononi, G., Fried, I., 2011. Sleep spindles in humans: insights from intracranial EEG and unit recordings. J. Neurosci. 31, 17821–17834.
Ayoub, A., Aumann, D., Hörschelmann, A., Kouchekmanesch, A., Paul, P., Born, J., Marshall, L., 2013. Differential effects on fast and slow spindle activity, and the sleep slow oscillation in humans with carbamazepine and flunarizine to antagonize voltage-dependent Na^+ and Ca^{2+} channel activity. Sleep 36, 905–911.
Bates, D., Mächler, M., Bolker, B., Walker, S., 2015. Fitting linear mixed-effects models using lme4. J. Stat. Softw. 67, 51.
Bazhenov, M., Timofeev, I., Steriade, M., Sejnowski, T.J., 2002. Model of thalamocortical slow-wave sleep oscillations and transitions to activated States. J. Neurosci. 22, 8691–8704.
Bazil, C.W., 2003. Effects of antiepileptic drugs on sleep structure: are all drugs equal? CNS Drugs 17, 719–728.
Beenhakker, M.P., Huguenard, J.R., 2009. Neurons that fire together also conspire together: is normal sleep circuitry hijacked to generate epilepsy? Neuron 62, 612–632.
Benjamini, Y., Hochberg, Y., 1995. Controlling the false discovery rate: a practical and powerful approach to multiple testing. J. R. Stat. Soc. Ser. B 57, 289–300.
Bonjean, M., Baker, T., Bazhenov, M., Cash, S., Halgren, E., Sejnowski, T., 2012. Interactions between core and matrix thalamocortical projections in human sleep spindle synchronization. J. Neurosci. 32, 5250–5263.
Cammoun, L., Gigandet, X., Meskaldji, D., Thiran, J.P., Sporns, O., Do, K.Q., Maeder, P., Meuli, R., Hagmann, P., 2012. Mapping the human connectome at multiple scales with diffusion spectrum MRI. J. Neurosci. Methods 203, 386–397.
Canolty, R.T., Edwards, E., Dalal, S.S., Soltani, M., Nagarajan, S.S., Kirsch, H.E., Berger, M.S., Barbaro, N.M., Knight, R.T., 2006. High gamma power is phase-locked to theta oscillations in human neocortex. Science 313, 1626–1628.
Cash, S.S., Halgren, E., Dehghani, N., Rossetti, A.O., Thesen, T., Wang, C., Devinsky, O., Kuzniecky, R., Doyle, W., Madsen, J.R., Bromfield, E., Eross, L., Halász, P., Karmos, G., Csercsa, R., Wittner, L., Ulbert, I., 2009. The human K-complex represents an isolated cortical down-state. Science 324, 1084–1087.
Clascá, F., Rubio-Garrido, P., Jabaudon, D., 2012. Unveiling the diversity of thalamocortical neuron subtypes. Eur. J. Neurosci. 35, 1524–1532.
Clemens, Z., Mölle, M., Eross, L., Jakus, R., Rásonyi, G., Halász, P., Born, J., 2011. Fine-tuned coupling between human parahippocampal ripples and sleep spindles. Eur. J. Neurosci. 33, 511–520.
Cobb, W.A., Guiloff, R.J., Cast, J., 1979. Breach rhythm: the EEG related to skull defects. Electroencephalogr. Clin. Neurophysiol. 47, 251–271.
Contreras, D., Destexhe, A., Sejnowski, T.J., Steriade, M., 1997. Spatiotemporal patterns of spindle oscillations in cortex and thalamus. J. Neurosci. 17, 1179–1196.
Csercsa, R., Dombovári, B., Fabó, D., Wittner, L., Eross, L., Entz, L., Sólyom, A., Rásonyi, G., Szucs, A., Kelemen, A., Jakus, R., Juhos, V., Grand, L., Magony, A., Halász, P., Freund, T.F., Maglóczky, Z., Cash, S.S., Papp, L., Karmos, G., Halgren, E., Ulbert, I., 2010. Laminar analysis of slow wave activity in humans. Brain 133, 2814–2829.
Daducci, A., Gerhard, S., Griffa, A., Lemkaddem, A., Cammoun, L., Gigandet, X., Meuli, R., Hagmann, P., Thiran, J.-P., 2012. The connectome mapper: an open-source processing pipeline to map connectomes with MRI. PLoS One 7, e48121.
Dale, A.M., Fischl, B., Sereno, M.I., 1999. Cortical surface-based analysis. I. Segmentation and surface reconstruction. Neuroimage 9, 179–194.
Davis, H., Davis, P.A., Loomis, A.L., Harvey, E.N., Hobart, G., 1937. Changes in human brain potentials during the onset of sleep. Science 86, 448–450.
De Gennaro, L., Ferrara, M., 2003. Sleep spindles: an overview. Sleep. Med. Rev. 7, 423–440.
Dehghani, N., Cash, S.S., Chen, C.C., Hagler, D.J., Huang, M., Dale, A.M., Halgren, E., 2010a. Divergent cortical generators of MEG and EEG during human sleep spindles suggested by distributed source modeling. PLoS One 5, e11454.
Dehghani, N., Cash, S.S., Halgren, E., 2011a. Emergence of synchronous EEG spindles from asynchronous MEG spindles. Hum. Brain Mapp. 32, 2217–2227.
Dehghani, N., Cash, S.S., Halgren, E., 2011. Topographical frequency dynamics within EEG and MEG sleep spindles. Clin. Neurophysiol. 122, 229–235.
Dehghani, N., Cash, S.S., Rossetti, A.O., Chen, C.C., Halgren, E., 2010b. Magnetoencephalography demonstrates multiple asynchronous generators during human sleep spindles. J. Neurophysiol. 104, 179–188.
Desikan, R.S., Ségonne, F., Fischl, B., Quinn, B.T., Dickerson, B.C., Blacker, D., Buckner, R.L., Dale, A.M., Maguire, R.P., Hyman, B.T., Albert, M.S., Killiany, R.J., 2006. An automated labeling system for subdividing the human cerebral cortex on MRI scans into gyral based regions of interest. Neuroimage 31, 968–980.
Diekelmann, S., Born, J., 2010. The memory function of sleep. Nat. Rev. Neurosci. 11, 114–126.
Dykstra, A.R., Chan, A.M., Quinn, B.T., Zepeda, R., Keller, C.J., Cormier, J., Madsen, J.R., Eskandar, E.N., Cash, S.S., 2012. Individualized localization and cortical surface-based registration of intracranial electrodes. Neuroimage 59, 3563–3570.
Ferrarelli, F., Huber, R., Peterson, M.J., Massimini, M., Murphy, M., Riedner, B.A., Watson, A., Bria, P., Tononi, G., 2007. Reduced sleep spindle activity in schizophrenia patients. Am. J. Psychiatry 164, 483–492.
Fischl, B., Sereno, M.I., Dale, A.M., 1999. Cortical surface-based analysis. II: Inflation, flattening, and a surface-based coordinate system. Neuroimage 9, 195–207.
Fogel, S.M., Smith, C.T., 2011. The function of the sleep spindle: a physiological index of intelligence and a mechanism for sleep-dependent memory consolidation. Neurosci. Biobehav. Rev. 35, 1154–1165.
Frauscher, B., von Ellenrieder, N., Dubeau, F., Gotman, J., 2015. Scalp spindles are associated with widespread intracranial activity with unexpectedly low synchrony. Neuroimage 105, 1–12.
Gibbs, F.A., Gibbs, E.L., 1950. Atlas of Electroencephalography 2nd ed.. Addison-Wesley Press, Cambridge, MA.
Gumenyuk, V., Roth, T., Moran, J.E., Jefferson, C., Bowyer, S.M., Tepley, N., Drake, C.L., 2009. Cortical locations of maximal spindle activity: magnetoencephalography (MEG) study. J. Sleep Res. 18, 245–253.
Hermes, D., Miller, K.J., Wandell, B.A., Winawer, J., 2015. Stimulus dependence of gamma oscillations in human visual cortex. Cereb. Cortex 25, 2951–2959.
Iber, C., Ancoli-Israel, S., Chesson, A.L., Quan, S.F., 2007. The AASM Manual for the Scoring of Sleep and Associated Events: Rules, Terminology, and Technical Specifications 1st ed.. American Academy of Sleep Medicine, Westchester, IL.
Jobert, M., Poiseau, E., Jähnig, P., Schulz, H., Kubicki, S., 1992. Topographical analysis of sleep spindle activity. Neuropsychobiology 26, 210–217.
Johnson, L.A., Blakely, T., Hermes, D., Hakimian, S., Ramsey, N.F., Ojemann, J.G., 2012. Sleep spindles are locally modulated by training on a brain-computer interface. Proc. Natl. Acad. Sci. USA 109, 18583–18588.
Jones, E.G., 2001. The thalamic matrix and thalamocortical synchrony. Trends Neurosci. 24, 595–601.
Kadipasaoglu, C.M., Baboyan, V.G., Conner, C.R., Chen, G., Saad, Z.S., Tandon, N., 2014. Surface-based mixed effects multilevel analysis of grouped human electrocorticography. Neuroimage 101, 215–224.
Lachaux, J.P., Rudrauf, D., Kahane, P., 2003. Intracranial EEG and human brain mapping. J. Physiol. Paris 97, 613–628.
Lüthi, A., 2013. Sleep spindles: where they come from, what they do. Neuroscientist 20, 243–256.
Mak-McCully, R.A., Rosen, B.Q., Rolland, M., Régis, J., Bartolomei, F., Rey, M., Chauvel, P., Cash, S.S., Halgren, E., 2015. Distribution, amplitude, incidence, co-occurrence,

and propagation of human K-complexes in focal transcortical recordings. eNeuro 2.
Malow, B.A., Carney, P.R., Kushwaha, R., Bowes, R.J., 1999. Hippocampal sleep spindles revisited: physiologic or epileptic activity? Clin. Neurophysiol. 110, 687–693.
Manshanden, I., De Munck, J.C., Simon, N.R., Lopes da Silva, F.H., 2002. Source localization of MEG sleep spindles and the relation to sources of alpha band rhythms. Clin. Neurophysiol. 113, 1937–1947.
Martin, N., Lafortune, M., Godbout, J., Barakat, M., Robillard, R., Poirier, G., Bastien, C., Carrier, J., 2013. Topography of age-related changes in sleep spindles. Neurobiol. Aging 34, 468–476.
Massimini, M., Huber, R., Ferrarelli, F., Hill, S., Tononi, G., 2004. The sleep slow oscillation as a traveling wave. J. Neurosci. 24, 6862–6870.
Montplaisir, J., Leduc, L., Laverdière, M., Walsh, J., Saint-Hilaire, J.M., 1981. Sleep spindles in the human hippocampus: normal or epileptic activity? Sleep 4, 423–428.
Mölle, M., Bergmann, T.O., Marshall, L., Born, J., 2011. Fast and slow spindles during the sleep slow oscillation: disparate coalescence and engagement in memory processing. Sleep 34, 1411–1421.
Mölle, M., Marshall, L., Gais, S., Born, J., 2002. Grouping of spindle activity during slow oscillations in human non-rapid eye movement sleep. J. Neurosci. 22, 10941–10947.
Nakabayashi, T., Uchida, S., Maehara, T., Hirai, N., Nakamura, M., Arakaki, H., Shimisu, H., Okubo, Y., 2001. Absence of sleep spindles in human medial and basal temporal lobes. Psychiatry Clin. Neurosci. 55, 57–65.
Nakamura, M., Uchida, S., Maehara, T., Kawai, K., Hirai, N., Nakabayashi, T., Arakaki, H., Okubo, Y., Nishikawa, T., Shimizu, H., 2003. Sleep spindles in human prefrontal cortex: an electrocorticographic study. Neurosci. Res. 45, 419–427.
Nir, Y., Staba, R.J., Andrillon, T., Vyazovskiy, V.V., Cirelli, C., Fried, I., Tononi, G., 2011. Regional slow waves and spindles in human sleep. Neuron 70, 153–169.
Nobili, L., De Gennaro, L., Proserpio, P., Moroni, F., Sarasso, S., Pigorini, A., De Carli, F., Ferrara, M., 2012. Local aspects of sleep: observations from intracerebral recordings in humans. Prog. Brain Res. 199, 219–232.
O'Reilly, C., Nielsen, T., 2014. Assessing EEG sleep spindle propagation. Part 2: experimental characterization. J. Neurosci. Methods 221, 215–227.
Peter-Derex, L., Comte, J.-C., Mauguière, F., Salin, P.A., 2012. Density and frequency caudo-rostral gradients of sleep spindles recorded in the human cortex. Sleep 35, 69–79.
Piantoni, G., Halgren, E., Cash, S.S., 2016. The Contribution of Thalamocortical Core and Matrix Pathways to Sleep Spindles. Neural Plast. 2016, 3024342.
Piantoni, G., Poil, S.-S., Linkenkaer-Hansen, K., Verweij, I.M., Ramautar, J.R., Van Someren, E.J.W., Van Der Werf, Y.D., 2013. Individual differences in white matter diffusion affect sleep oscillations. J. Neurosci. 33, 227–233.
Pinheiro, J.C., Bates, D.M., 2000. Mixed Effects Models in S and S-Plus, Statistics and Computing. Springer, New York, NY.
R Development Core Team, 2010. R: A Language and Environment for Statistical Computing. R Foundation for Statistical Computing, Vienna, Austria.
Rosanova, M., Casali, A., Bellina, V., Resta, F., Mariotti, M., Massimini, M., 2009. Natural frequencies of human corticothalamic circuits. J. Neurosci. 29, 7679–7685.
Rosanova, M., Ulrich, D., 2005. Pattern-specific associative long-term potentiation induced by a sleep spindle-related spike train. J. Neurosci. 25, 9398–9405.
Sarasso, S., Proserpio, P., Pigorini, A., Moroni, F., Ferrara, M., De Gennaro, L., De Carli, F., Lo Russo, G., Massimini, M., Nobili, L., 2014. Hippocampal sleep spindles preceding neocortical sleep onset in humans. Neuroimage 86, 425–432.
Schabus, M., Dang-Vu, T.T., Albouy, G., Balteau, E., Boly, M., Carrier, J., Darsaud, A., Degueldre, C., Desseilles, M., Gais, S., Phillips, C., Rauchs, G., Schnakers, C., Sterpenich, V., Vandewalle, G., Luxen, A., Maquet, P., 2007. Hemodynamic cerebral correlates of sleep spindles during human non-rapid eye movement sleep. Proc. Natl. Acad. Sci. USA 104, 13164–13169.
Siclari, F., Bernardi, G., Riedner, B.A., LaRocque, J.J., Benca, R.M., Tononi, G., 2014. Two distinct synchronization processes in the transition to sleep: a high-density electroencephalographic study. Sleep 37, 1621–1637.
Simons, J.S., Spiers, H.J., 2003. Prefrontal and medial temporal lobe interactions in long-term memory. Nat. Rev. Neurosci. 4, 637–648.
Steriade, M., McCormick, D.A., Sejnowski, T.J., 1993a. Thalamocortical oscillations in the sleeping and aroused brain. Science 262, 679–685.
Steriade, M., Nuñez, A., Amzica, F., 1993b. A novel slow (< 1 Hz) oscillation of neocortical neurons in vivo: depolarizing and hyperpolarizing components. J. Neurosci. 13, 3252–3265.
Urakami, Y., 2008. Relationships between sleep spindles and activities of cerebral cortex as determined by simultaneous EEG and MEG recording. J. Clin. Neurophysiol. 25, 13–24.
Valderrama, M., Crépon, B., Botella-Soler, V., Martinerie, J., Hasboun, D., Alvarado-Rojas, C., Baulac, M., Adam, C., Navarro, V., Le Van Quyen, M., 2012. Human gamma oscillations during slow wave sleep. PLoS One 7, e33477.
Wennberg, R., Cheyne, D., 2013. On noninvasive source imaging of the human K-complex. Clin. Neurophysiol. 124, 941–955.
Werth, E., Achermann, P., Dijk, D.J., Borbély, A.A., 1997. Spindle frequency activity in the sleep EEG: individual differences and topographic distribution. Electroencephalogr. Clin. Neurophysiol. 103, 535–542.